Applied Physics B (2022) 128:158
https://doi.org/10.1007/s00340-022-07880-1

Applied Physics B
Lasers and Optics

Simplified highly sensitive temperature sensor based on harmonic Vernier effect

Liqin Xie[1] · Mengmeng Chen[2] · Zuxing Zhang[1]

Received: 18 March 2022 / Accepted: 22 July 2022 / Published online: 1 August 2022

Abstract

A highly sensitive temperature sensor with cascaded polarization maintaining fiber–Sagnac interferometers (PMF–SIs) based on harmonic Vernier effect has been proposed and experimentally demonstrated. Both simulation and experiment results indicate that the fundamental Vernier effect can be achieved through cascading two PMF–SIs with similar free spectral ranges (FSRs) and the first-order harmonic Vernier effect can be further realized by two PMF–SIs possessing FSRs with an approximate multiple relationship. The maximum sensitivity of the cascaded PMF–SIs based on harmonic Vernier effect has be enhanced about 35.5 times compared with that of single PMF–SI, exhibiting a high temperature sensitivity of − 53.3 nm/°C in the temperature measurement range from 30 to 37 °C. The temperature sensor with simple structure and high sensitivity has a great application prospect.

1 Introduction

Temperature sensing is one of the most fundamental and significant applications of fiber devices, which can be applied to industrial manufacturing, biomedical science, fuel storage and so on. In recent years, due to compact structure and convenient manufacturing of optical fiber sensors, researchers vigorously develop optical fiber sensors for temperature monitoring. Currently, fiber grating [1–4], hollow core fiber (HCF) [5–8] and other specific fibers [9–13] are commonly used materials for manufacturing optical fiber temperature sensors. The technical requirements and rapid development of many research fields have brought greater pressure to the current optical fiber sensing research and proposed new challenges. Compared with conventional optical fiber sensors, there is an increasing demand for sensing structures that can achieve higher sensitivity and resolution. However, limited by the responsivity of the optical fiber material, the sensitivity of the structure can hardly raise dramatically. Therefore, researchers are forced to find new solutions for sensitivity-enhanced fiber optic sensors.

This issue could hopefully be solved by assembling two structures, which, respectively, regarded as the fixed part and the sliding part of the Vernier caliper, with slightly different free spectral ranges (FSRs) to induce the Vernier effect. To obtain higher sensitivity, the application of the Vernier effect has emerged [14–20]. By comparison with a single structure, the sensitivity of the cascaded structure can be improved several times. In 2015, Shao et al. proposed a fiber optic temperature sensor using two cascaded Sagnac interferometers, which consisted of polarization maintaining fibers (PMFs) with slightly different lengths. Experimental results reveal that the temperature sensitivity is enhanced from 1.46 nm/°C of single Sagnac configuration to 13.36 nm/°C [21]. In 2017, Xu et al. proposed and experimentally demonstrated a temperature sensor employing the Vernier effect generated from a cascaded fiber ring-based microwave photonic filter (MPF). The sensitivity of the cascaded fiber ring-based sensor can be improved about 30 times compared with the single fiber ring-based temperature sensor [22]. In 2018, Li et al. proposed and achieved an optical cascaded Fabry–Perot interferometer (FPI) hydrogen sensor. The hydrogen sensitivity is − 1.04 nm/% within the range of 0–2.4%, which is greatly improved because of the Vernier effect [23]. In addition, in 2018, Zhang et al. proposed a temperature sensor based on two cascaded FPIs for ultrahigh sensitivity temperature

✉ Mengmeng Chen
chenmm@njxzc.edu.cn

✉ Zuxing Zhang
zxzhang@njupt.edu.cn

1 Advanced Photonic Technology Lab, College of Electronic and Optical Engineering, Nanjing University of Posts and Telecommunications, Nanjing 210023, China

2 School of Electronic Engineering, Nanjing Xiaozhuang University, Nanjing 211171, China

sensing, which reached 67 nm/°C. In 2021, Ding et al. enhanced the temperature sensitivity from − 2.24 nm/°C of single polarization maintaining fiber–Sagnac interferometer (PMF–SI) to − 23.68 nm/°C of cascaded configuration with an enhancement factor of 10.6.

The above mentioned works are all based on the fundamental optical Vernier effect. In 2019, Gomes et al. proposed the concept of harmonic Vernier effect for the first time [24]. By comparison to the previous method, the FSRs of the two structures are not required to be close. At the same time, as the order of harmonics increases, the sensitivity amplification factor also increases by multiple times, making it feasible to break through the limitations of the traditional fundamental Vernier effect. In 2020, Gomes et al. utilized hollow microsphere and a section of fiber as two FPIs to generate the optical Vernier effect. This effect generates higher magnification factors, proportional to the order of the harmonics [25]. Recently, Yang et al. proposed a simple gas pressure sensor by fusion splicing two hollow silica capillaries as FPIs. By properly adjusting the length of the silica capillaries, harmonic of optical Vernier effect is observed. The results showed a sensitivity of 80.8 pm/kPa from 1 to 101 kPa with good linearity of 99.7% [26]. Nevertheless, FPIs possess extremely poor temperature sensitivity owing to the air cavity structure. Moreover, FPIs have relatively fine requirements for the cavity length, which is generally in the order of micrometers. The control of the length is strict and the operation is more troublesome.

In this paper, we combine a simple temperature sensing structure with an optical sensitivity magnification, through the harmonics of the Vernier effect. Both theoretical and experimental consequences have verified the harmonic optical Vernier effect, and the influence of the FSR's difference on the magnification factor has also been investigated. The highest sensitivity of − 53.3 nm/°C of the proposed sensor consisting of cascaded PMF–SIs, in temperature measurement range from 30 to 37 °C, 35.5 times sensitivity enhancement in comparison with single PMF–SI, has been reached.

2 Theory and simulation

Considering the case of single PMF–SI, the light splits into two beams passing after through the 3 dB coupler. When two beams pass through the PMF, the birefringence effect of the PMF will cause the optical path difference of the two beams. When they meet again at the 3 dB coupler, the optical path difference can lead to interference phenomenon. Furthermore, the FSR of single PMF–SI can be conjectured as

$$\mathrm{FSR} = \lambda^2 / BL \tag{1}$$

where L is the effective length of the tapered part, and λ is the central wavelength of the light source. B represents the refractive index difference of slow and fast axes ($B = n_{\mathrm{slow}} = n_{\mathrm{fast}}$), which is a fixed value 3.5×10^{-4} for our used PMF (Nufern PM1550-XP). From the formula, it can be seen that L is inversely proportional to FSR. When the length of PMF is longer, FSR is smaller. Then we consider the two cascaded PMF–SIs as sensing and reference PMF–SIs, respectively, whose FSRs (FSR_1 and FSR_2) are expressed as

$$\mathrm{FSR}_1 = \frac{\lambda^2}{BL_1}, \quad \mathrm{FSR}_2 = \frac{\lambda^2}{BL_2} \tag{2}$$

When the FSRs of the two interferometers satisfy the Vernier condition: $\mathrm{FSR}_1 = (i+1) \cdot \mathrm{FSR}_2 \pm \Delta\mathrm{FSR}, \quad i = 0,\ 1,\ 2...$, $\Delta\mathrm{FSR}$ is the difference between FSR_1 and FSR_2, the cascaded structure can bring the optical Vernier effect. It is the fundamental Vernier effect when $i = 0$. In other cases, it is the harmonic Vernier effect, and i represents the order of harmonics. When the transmission peaks of the two periodic comb spectra coincide, the maximum transmittance can be obtained. Since $\Delta\mathrm{FSR}$ is small, the transmission peaks will overlap again after several orders of magnitude, resulting in periodic envelopes in the spectra after the cascade. The FSR of the upper envelope of the cascaded PMF–SIs sensor can be deduced as [24]

$$\mathrm{FSR}^{i}_{\mathrm{envelope}} = \frac{\mathrm{FSR}_1 \cdot \mathrm{FSR}_2}{\left|\mathrm{FSR}_1 - (i+1)\mathrm{FSR}_2\right|} \tag{3}$$

Different from the fundamental optical Vernier effect, we regard the period of the inner envelope (FSRc) as the FSR of the cascade structure when the sensor operates under the harmonic Vernier effect. The FSR is related to the order of harmonics [21], which can be expressed as

$$\mathrm{FSR}^{i}_{\mathrm{C}} = \frac{(i+1)\mathrm{FSR}_1 \cdot \mathrm{FSR}_2}{\left|\mathrm{FSR}_1 - (i+1)\mathrm{FSR}_2\right|} \tag{4}$$

The slight drift of the sensing PMF–SI spectrum will cause the position of the previously aligned transmission peak to change greatly, thereby changing the spectrum of the cascade structure. Under the influence of the fundamental Vernier effect, the offset of the cascaded structure will be several times larger than that of a single structure. The magnification factor is [16]

$$M^0 = \frac{\mathrm{FSR}^{0}_{\mathrm{envelope}}}{\mathrm{FSR}_1} = \frac{\mathrm{FSR}_2}{\left|\mathrm{FSR}_1 - \mathrm{FSR}_2\right|} \tag{5}$$

While for the harmonic Vernier effect, the magnification is not only related to the FSRs of the two PMFs, but also related to the order. The magnification factor based on the harmonics of the optical Vernier effect is

$$M^i = \frac{\mathrm{FSR}_C^i}{\mathrm{FSR}_1} = \frac{(i+1)\mathrm{FSR}_2}{\left|\mathrm{FSR}_1 - (i+1)\mathrm{FSR}_2\right|} \tag{6}$$

It is $i+1$ times the sensitivity with fundamental harmonic Vernier effect. To verify the theory, the fundamental and the first harmonic Vernier effects have been simulated. For the fundamental Vernier effect, set $\mathrm{FSR}_1 = 26.8$ nm, $\mathrm{FSR}_2 = 28.4$ nm, in this case, $i = 0$, $\Delta\mathrm{FSR} = 1.6$ nm. According to the theoretical analysis and Eq. (3), the theoretical $\mathrm{FSR}^0_{\mathrm{envelope}}$ is about 476 nm. For the first harmonic Vernier effect, set $\mathrm{FSR}_1 = 26.8$ nm, $\mathrm{FSR}_2 = 14.2$ nm, in this case, $i = 1$, $\Delta\mathrm{FSR} = 1.6$ nm. According to the theoretical analysis and Eq. (4), the theoretical $\mathrm{FSR}^1_{\mathrm{envelope}}$ is about 238 nm and FSR^1_c is about 476 nm. The simulated transmission spectra obtained are shown in Fig. 1.

To investigate the effect of the $\Delta\mathrm{FSR}$ on FSR^1_c, FSR_1 is kept constant 26.8 nm and FSR_2 is increased, resulting in the expanding $\Delta\mathrm{FSR}$. With the FSR_2 increased from 13.8 nm to 14.2 nm and 14.9 nm, the corresponding $\Delta\mathrm{FSR}$ is increased from 0.8 nm to 1.6 nm and 3 nm, the transmission spectra of the cascaded structures are shown in Fig. 2. It can be seen that the simulation result is consistent with that of the theoretical results, and the conclusion is that the smaller the $\Delta\mathrm{FSR}$, the larger the FSR^i_c, and similarly, the corresponding magnification factor of M^i will be larger.

3 Experiment and results

The experimental setup for temperature measurement is schematically depicted in Fig. 3. A broadband source (BBS) with wavelength range from 1250 to 1650 nm is adopted as light source of the sensing schemes. A column oven is used to change the ambient temperature. As the temperature of oven changes from 30 to 38 ℃ with a step size of 1 ℃, the spectrum measurement is illustrated and saved via an optical spectrum analyzer (OSA) individually. For Vernier-based configuration, only one of PMF–SIs is placed in the oven, the other PMF–SI acts as a reference at room temperature.

According to the experimental setup diagram, the temperature sensitivity of the single PMF–SI-based sensor is first investigated. The PMF length of sensing PMF–SI is about

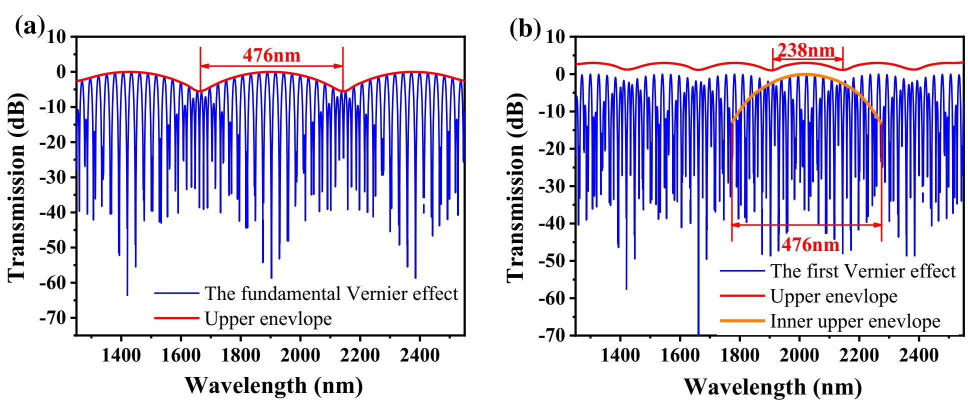

Fig. 1 Simulated transmission spectra of the cascaded structures based on a fundamental Vernier effect, **b** first harmonic Vernier effect (red line is the upper envelope, and orange line is the inner upper envelope)

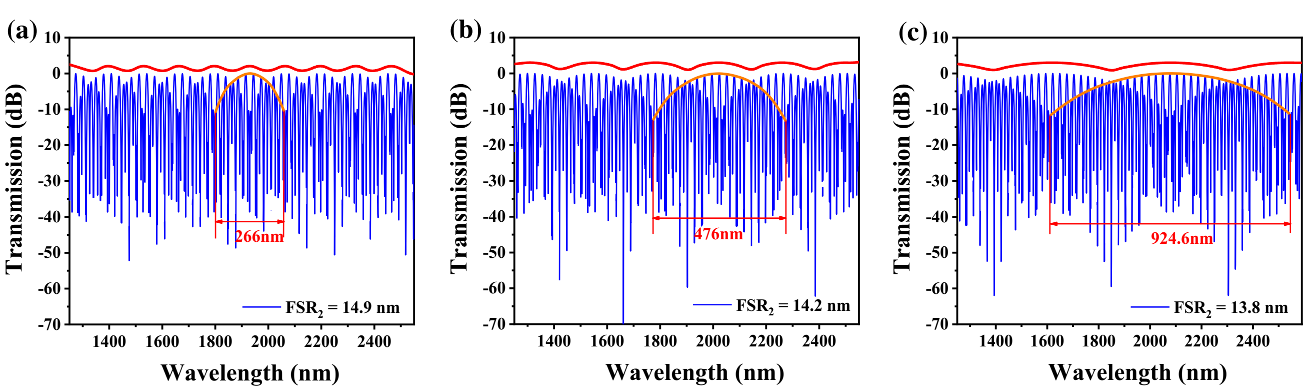

Fig. 2 Transmission spectra of the cascaded structures with different FSR2 (red line is the upper envelope, and orange line is the inner upper envelope)

25.5 cm, and the FSR is 26.88 nm, as shown in Fig. 4a. The spectrum has a blue shift when the temperature increases. As it can be seen from the linear fitting red curve in Fig. 4b, the temperature sensitivity of the single PMF–SI-based sensor, is − 1.5 nm/℃ with R-square of 0.99945.

In the experiment based on the fundamental optical Vernier effect, the PMF length of the two PMF–SIs is required to be close. The sensing PMF–SI is the same one as the single PMF–SI sensor, with PMF length of about 25.5 cm and the FSR of 26.88 nm. Thus, the length of the reference PMF is chosen to be 24 cm. As shown in Fig. 5a, the FSR of the reference PMF–SI is 28.5 nm. The reference PMF–SI is exposed in air to maintain room temperature and the sensing PMF–SI is placed in oven to monitor the changing temperature. As indicated in Fig. 5b, the dip of the upper envelope is regarded as the reference point. The upper envelope is denoted by a red line, and the reference point is represented by an arrow. Similarly, as the temperature gradually rises from 30 to 38 ℃ with a step size of 1 ℃, the arrowed point drifts to the left. From the red fitting curve in Fig. 5c, it can

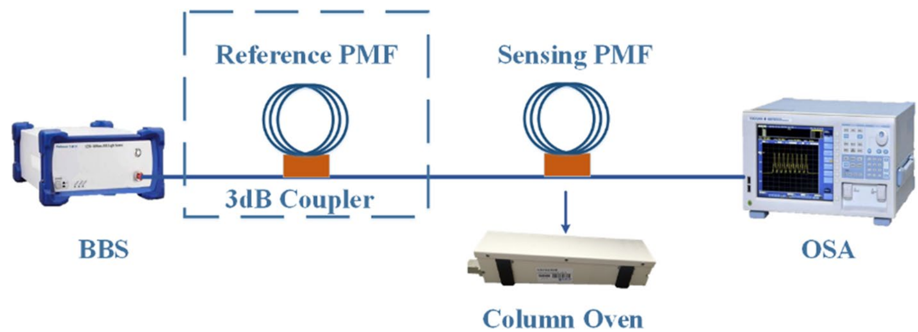

Fig. 3 Experiment setup of temperature measurement

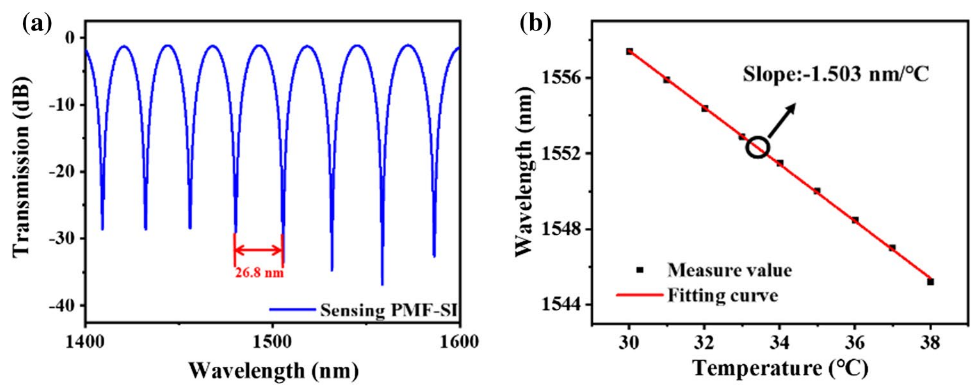

Fig. 4 **a** Transmission spectrum of the sensing PMF–SI, **b** linear fitting result of wavelength shift versus temperature for single PMF–SI

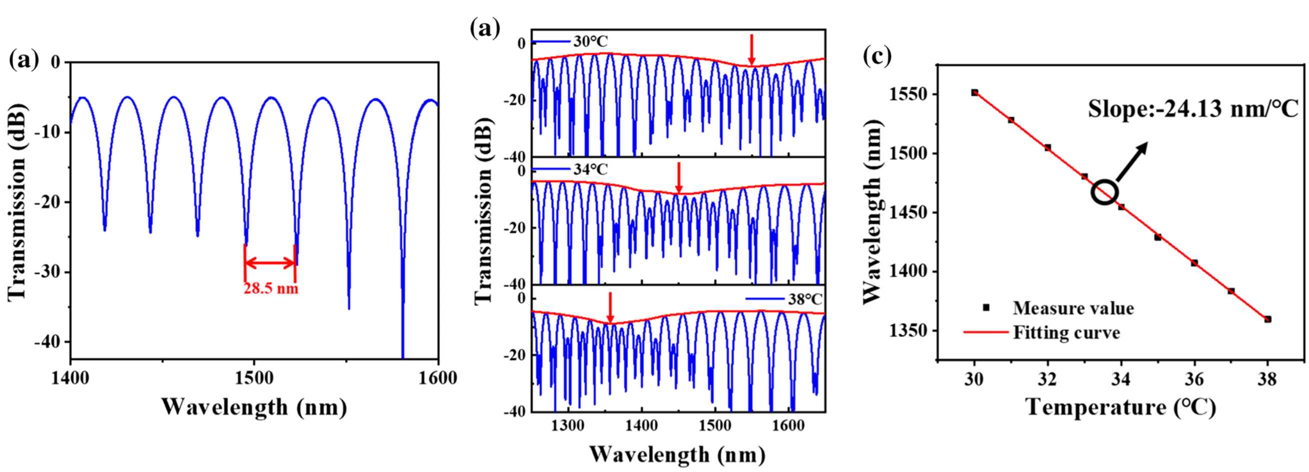

Fig. 5 **a** Transmission spectrum of the reference PMF–SI, **b** transmission spectra with temperature rises (red line is the fitted upper envelope), **c** linear fitting of wavelength shift versus temperature for the cascaded PMF–SIs based on fundamental optical Vernier effect

be known that the temperature sensitivity of the sensor based on fundamental optical Vernier effect is − 24.1 nm/°C. Apparently, the sensitivity of the cascaded PMF–SI-based sensor is much higher than that of a single PMF–SI-based sensor, exhibiting a sensitivity enhancement factor of 16.1.

To explore the temperature sensitivity of the sensor based on harmonic optical Vernier effect and the influence of ΔFSR on the experimental results, we fabricated three reference PMF–SI samples (samples 1–3) with different length, which is increased from 46 to 50 cm. The corresponding FSRs of the three reference PMF–SIs are 14.9 nm, 14.2 nm and 13.8 nm, respectively, as shown in Fig. 6. The ΔFSR are 2.9 nm, 1.5 nm and 0.7 nm, respectively.

The reference PMF–SIs were, respectively, cascaded with the sensing structure, and the superimposed spectra are observed, as shown in Fig. 7a. By fitting the inner upper envelope of the three spectra, it can be seen that the larger the ΔFSR, the smaller the FSR_c^1, and the FSR_c^1 of proposed sensor with sample 3 is the biggest. When the temperature of the column oven increases, the three spectra appear blue shift, which is dependent upon the ΔFSR. As depicted in Fig. 7b, the temperature sensitivity of the cascaded PMF–SI-based sensors with three samples, are − 15.5 nm/℃, − 27.9 nm/℃ and − 53.3 nm/℃, respectively. In contrast, temperature sensitivity of single PMF–SI is − 1.5 nm/℃. Distinctly, the sensitivity of the cascaded PMF–SI-based sensor is much higher than that of a single PMF–SI-based sensor, exhibiting a maximum sensitivity enhancement factor of 35.5. Noted that this technology can be used for any temperature detection, although highly sensitive detection was achieved only in the temperature range of 30–37 °C in this work. Due to the large FSR of the interference spectral envelope wave generated by the sensing device based on the harmonic Vernier effect, the temperature range that can be monitored is limited. Since when the wavelength drift is too large, the available wavelength range of the broadband light source or the measurable wavelength range of the optical spectrum analyzer will be exceeded. Moreover, the sensor has a high resolution determined by the resolution of the spectrometer used for demodulation.

The proposed sensor consisting of two PMF–SIs, is rather easy to implement, not involving any expensive equipment

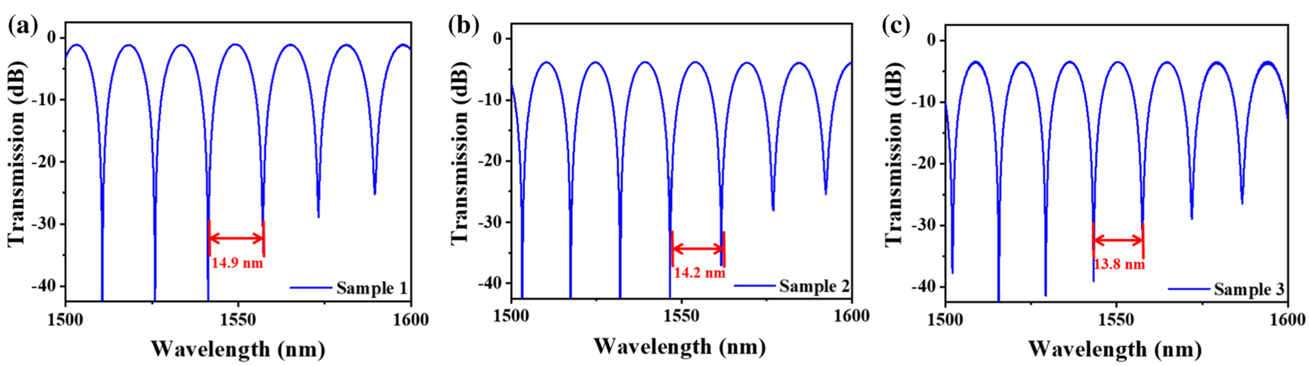

Fig. 6 Transmission spectrum of the reference PMF–SIs for the first harmonic Vernier effect **a** sample 1, **b** sample 2, **c** sample 3

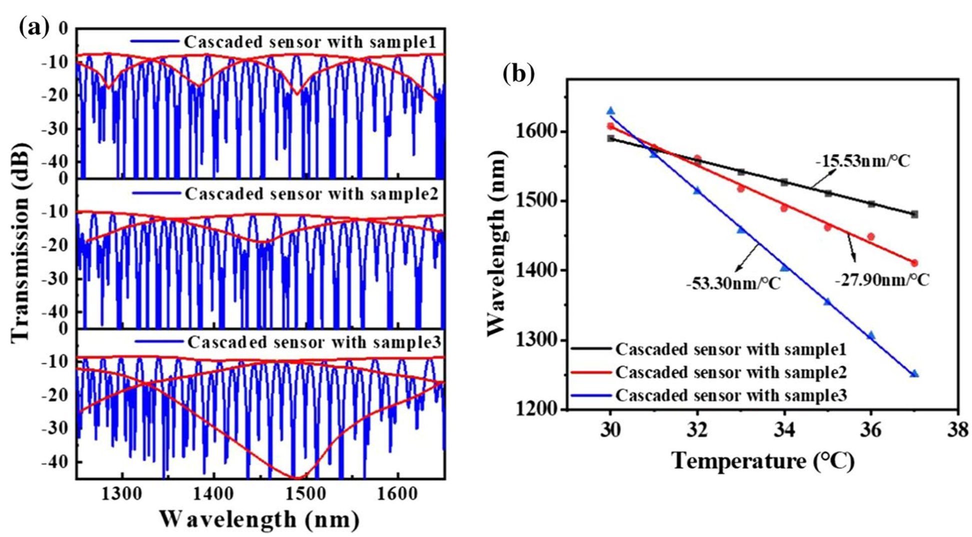

Fig. 7 **a** Transmission spectra of cascaded PMF–SI-based sensors with sample1–sample3 (red line is the fitted inner upper envelope), **b** linear fitting results of wavelength shift versus temperature

Table 1 Comparison between the proposed sensor and the reported works

Structure	Sensitivity (nm/°C)	References
Cascaded PMF–SIs	− 43	[27]
Cascaded PMF–SIs	− 23.68	[28]
Cascaded PMF–SIs	3.66 nm	[29]
Cascaded PMF–SI and MZI	20.86	[30]
Cascaded PMF–SIs	− 53.3	This work

or complex procedures, but features high sensitivity and low-cost. To highlight the advantages of the proposed sensor, it is essential to give some comparisons between the proposed sensor and several representative works employed Vernier effect of cascaded PMF–SIs, as shown in Table 1. It can be seen from Table 1 that the temperature sensitivity of our proposed sensor with the first order optical Vernier effect is comparatively high (up to − 53.3 nm/°C) without adding any structural complexity, which is more than 2 times that of the cascaded PMF–SIs sensor based on the fundamental optical Vernier effect.

4 Conclusions

A sensitivity enhanced temperature sensor with PMF–SIs based on the Vernier effect has been proposed and demonstrated in this paper. Though exploring the fundamental and the first harmonic Vernier effects through both simulations and experiments, results confirmed that the smaller the ΔFSR, the larger the FSR_c^i, and similarly, the corresponding magnification factor of FSR_c^i will be larger. The proposed temperature sensor exhibits − 53.3 nm/°C of sensitivity in the temperature measurement range of 30–37 °C, with 35.5 times sensitivity enhancement. The proposed sensor with high sensitivity, easy fabrication and low cost has potential applications that need precise and remote temperature control, such as lasers, biochemical engineering, medical treatment, and nuclear test.

Acknowledgements We acknowledge the supports from National Natural Science Foundation of China under Grant 91950105 and 62105157, Jiangsu Postdoctoral Research Funding Program (2021K228B), Natural Science Funding of Jiangsu Province (BK20211014), and 1311 Talent Plan of Nanjing University of Posts and Telecommunications.

References

1. D. Polito, M.A. Caponero, A. Polimadei, P. Saccomandi, C. Massaroni, S. Silvestri, E. Schena, A needle-like probe for temperature monitoring during laser ablation based on fiber Bragg grating: manufacturing and characterization. J. Med. Device **9**(4), 041006 (2015)
2. X.K. Gao, T.G. Ning, C.B. Zhang, J. Xu, J.J. Zheng, H. Lin, J. Li, L. Pei, H.D. You, A dual-parameter fiber sensor based on few-mode fiber and fiber Bragg grating for strain and temperature sensing. Opt. Commun. **454**, 124441 (2020)
3. B.W. Zhang, M. Kahrizi, High-temperature resistance fiber Bragg grating temperature sensor fabrication. IEEE Sens. J. **7**(4), 586–591 (2007)
4. U. Sampath, D.G. Kim, H.J. Kim, M.H. Song, Polymer-coated FBG sensor for simultaneous temperature and strain monitoring in composite materials under cryogenic conditions. Appl. Opt. **57**(3), 492–497 (2018)
5. R. Zeltner, R. Pennetta, S.R. Xie, P.S.J. Russell, Flying particle microlaser and temperature sensor in hollow-core photonic crystal fiber. Opt. Lett. **43**(7), 1479–1482 (2018)
6. H.L. Wang, A.J. Yang, Temperature sensing property of hollow-core photonic bandgap fiber filled with CdSe/ZnS quantum dots in an UV curing adhesive. Opt. Fiber Technol. **38**(5), 104–107 (2017)
7. B. Feng, Y. Liu, S.L. Qu, High-temperature sensor based on resonant reflection in hollow core fiber. Opt. Eng. **55**(10), 106127 (2016)
8. S. Hao, L. Hao, W. Xin, L. Liang, Y.C. Wang, X.C. Ma, J.Q. Zhang, M.L. Hu, X.G. Qiao, Spectrum ameliorative optical fiber temperature sensor based on hollow-core fiber and inner zinc oxide film. Sens. Actuators, B Chem. **245**, 423–427 (2017)
9. X.T. Ren, J. Gao, H.N. Shi, L.H. Huang, S.L. Zhao, S.Q. Xu, A highly sensitive all-fiber temperature sensor based on the enhanced green upconversion luminescence in Lu2MoO6:Er3+/Yb3+ phosphors by co-doping Li+ ions. Optik Int. J. Light Electron Opt. **227**, 166084 (2021)
10. L.V. Nguyen, D.S. Hwang, S. Moon, D.S. Moon, Y. Chung, High temperature fiber sensor with high sensitivity based on core diameter mismatch. Opt. Express **16**(15), 11369–11375 (2018)
11. C.T. Wang, C.Y. Wang, J.H. Yu, I.T. Kuo, C.W. Tseng, H.C. Jau, Y.J. Chen, T.H. Lin, Highly sensitive optical temperature sensor based on a SiN micro-ring resonator with liquid crystal cladding. Opt. Express **24**(2), 1002–1007 (2016)
12. Q.Z. Sun, X.H. Sun, W.H. Jia, Z.L. Xu, H.P. Luo, D.M. Liu, L. Zhang, Graphene assisted microfiber for optical-power-based temperature sensor. IEEE Photon. Technol. Lett. **28**(4), 383–386 (2016)
13. J.F. Zhao, P.P. Niu, C. Zhang, H. Bai, X.D. Sun, Z.B. Han, Simultaneous refractive index and temperature measurement using nested fiber balloon rings. Appl. Opt. **57**(23), 6835–6839 (2018)
14. L. Jin, M.Y. Li, J.J. He, Highly-sensitive silicon-on-insulator sensor based on two cascaded micro-ring resonators with Vernier effect. Opt. Commun. **284**, 156–159 (2011)
15. Z.L. Xua, Q.Z. Sun, W.H. Jia, P.P. Shum, D.M. Liu, Highly sensitive refractive index sensor based on two cascaded microfiber knots with Vernier effect. Opt. Express **23**(5), 6226–6229 (2015)
16. P. Zhang, M. Tang, F. Gao, B.P. Zhu, S.N. Fu, J. Ouyang, P.P. Shum, D.M. Liu, Cascaded fiber-optic Fabry-Perot interferometers with Vernier effect for highly sensitive measurement of axial strain and magnetic field. Opt. Express **22**(16), 19581–19588 (2014)
17. J.J. Tian, Z.G. Li, Y.X. Sun, Y. Yao, High-sensitivity fiber-optic strain sensor based on the Vernier effect and separated Fabry-Perot interferometers. J. Lightw. Technol. **37**(21), 5609–5618 (2019)
18. P.F. Wang, Y. Jiang, Y. Yi, G. Brambilla, Ultra-high-sensitivity refractive index sensor based on dual-microfiber coupler structure with the Vernier effect. Opt. Lett. **45**(5), 1268–1271 (2020)
19. Y.X. Zhang, B. Xu, D.N. Wang, H.P. Gong, Y. Li, C.L. Zhao, Sensitivity-enhanced fiber strain sensing system based on microwave

frequency scanning with the Vernier effect. Opt. Fiber Technol. **43**, 175–179 (2018)
20. Q.H. Wang, X. Liu, D.N. Wang, Ultra-sensitive gas pressure sensor based on Vernier effect with controllable amplification factor. Opt. Fiber Technol. **61**, 102404 (2021)
21. L.Y. Shao, Y. Luo, Z.Y. Zhang, X.H. Zou, B. Luo, W. Pan, L.S. Yan, Sensitivity-enhanced temperature sensor with cascaded fiber optic Sagnac interferometers based on Vernier-effect. Opt. Commun. **336**, 73–76 (2015)
22. Z.W. Xu, X.W. Shu, H.Y. Fu, Sensitivity enhanced fiber sensor based on a fiber ring microwave photonic filter with the Vernier effect. Opt. Express **25**(18), 20559–21566 (2017)
23. Y.N. Li, C.L. Zhao, B. Xu, D.N. Wang, M.H. Yang, Optical cascaded Fabry-Perot interferometer hydrogen sensor based on Vernier effect. Opt. Commun. **414**, 166–171 (2018)
24. A.D. Gomes, M.S. Ferreira, J. Bierlich, J. Kobelke, M. Rothhardt, H. Bartelt, O. Frazao, Optical harmonic Vernier effect: a new tool for high performance interferometric fiber sensors. Sensors **19**(24), 5431 (2019)
25. A.D. Gomes, M.S. Ferreira, J. Bierlich, J. Kobelke, M. Rothhardt, H. Bartelt, O. Frazao, Hollow microsphere combined with optical harmonic Vernier effect for strain and temperature discrimination. Opt. Laser Technol. **127**, 106198 (2020)
26. X.M. Yang, S. Wu, H.H. Cheng, J.W. Ma, S. Wang, S.H. Liu, P.X. Lu, Simplified highly-sensitive gas pressure sensor based on harmonic Vernier effect. Opt. Laser Technol. **140**, 107007 (2021)
27. Z.C. Ding, Z.W. Tan, P.K. Zhang, L.W. Zhang, Highly sensitive temperature sensor based on cascaded HiBi-FLMs with the Vernier effect. J. Opt. Soc. Am. B **37**(7), 1948–1955 (2020)
28. Z.C. Ding, Z.W. Tan, S.Y. Xiao, H.P. Gao, Sensitivity amplification of high birefringence fiber loop mirror temperature sensor with Vernier effect. Appl. Phys. B **127**(5), 63 (2021)
29. S. Liu, G.W. Liu, D.Y. Lv, M.M. Chen, Z.X. Zhang, Sensitivity enhanced temperature sensor with cascaded Sagnac loops based on harmonic Vernier effect. Opt. Fiber Technol. **66**, 102654 (2021)
30. W.D. Luo, Z.G. Cao, G.S. Zhang, F.Y. Liu, B. Liu, W.Y. Du, Y.H. Han, B.L. Yu, A highly sensitive optical fiber temperature sensor based on the enhanced Vernier effect. Opt. Fiber Technol. **67**, 102702 (2021)